

Solving the m -mixing problem for the three-dimensional time-dependent Schrödinger equation by rotations: application to strong-field ionization of H_2^+

T. K. Kjeldsen, L. A. A. Nikolopoulos, and L. B. Madsen

Lundbeck Foundation Theoretical Center for Quantum System Research,

Department of Physics and Astronomy, University of Aarhus, 8000 Aarhus C, Denmark.

We present a very efficient technique for solving the three-dimensional time-dependent Schrödinger equation. Our method is applicable to a wide range of problems where a fully three-dimensional solution is required, i.e., to cases where no symmetries exist that reduce the dimensionality of the problem. Examples include arbitrarily oriented molecules in external fields and atoms interacting with elliptically polarized light. We demonstrate that even in such cases, the three-dimensional problem can be decomposed exactly into two two-dimensional problems at the cost of introducing a trivial rotation transformation. We supplement the theoretical framework with numerical results on strong-field ionization of arbitrarily oriented H_2^+ molecules.

PACS numbers: 02.70.-c, 33.80.Rv

I. INTRODUCTION

In atomic physics the spherical symmetry of atoms promotes the spherical coordinates to a special position. The three independent variables are (r, θ, ϕ) , with r the radial distance of the electron with respect to the nucleus, θ the polar angle and ϕ the azimuthal angle. The Schrödinger equation for the hydrogen atom is separable in these coordinates with wave functions of the form $\psi_{nlm}(\mathbf{r}) = R_{nl}(r)Y_{lm}(\theta, \phi)$ separated into a radial wave function $R_{nl}(r)$ and a spherical harmonic $Y_{lm}(\theta, \phi)$. Furthermore, configurations of this type with associated orbitals $\psi_{nlm}(\mathbf{r})$ form the building blocks of Slater determinants and consequently of mean field approaches to atomic structure. Even for molecules where the presence of multiple nuclei breaks the spherical symmetry ($[L^2, H] \neq 0$), single-centre expansions in spherical harmonic basis has been used successfully [1].

For a general problem involving a single active electron we are thus led to the consideration of the three-dimensional time-dependent Schrödinger equation in spherical coordinates and for the reduced wave function ($\Phi = r\Psi$) we seek a solution of the form

$$\Phi(\mathbf{r}, t) = \sum_{l=0}^{\infty} \sum_{m=-l}^l f_{lm}(r, t) Y_{lm}(\theta, \phi). \quad (1)$$

A very important advantage of this representation is that we can benefit from angular momentum theory when dealing with the angular degrees of freedom. An outstanding problem, however, remains. The problem, which is referred to as the m -mixing problem among computational scientists, is that often couplings—external or internal—are present that introduce a mixing of m 's across l 's. Such m -mixings occur for example when an atom is subject to an elliptically polarized field or to a linearly polarized field described beyond the dipole approximation. When m is no longer conserved, the dynamics affects all three coordinates and a numerical simulation is difficult: three-dimensional calculations tend to be ex-

tremely time-consuming and computationally demanding.

In the course of our recent work concerned with alignment-dependent response of molecules to strong external fields we found a solution that speeds up the calculation by the use of an exact mapping of the three-dimensional problem to two two-dimensional problems. In the following we discuss the method by the specific example of the response of an arbitrarily oriented diatomic molecule to an external perturbation so strong that the system is ionized. As will become clear, the central ideas are completely general and carry over to the related case of atoms in elliptically polarized fields, polyatomic molecules as well as m -problems in geology and astronomy where expansions in spherical harmonics are also often encountered.

The paper is organized as follows: in Sec. II we give an overview over the basic idea of our technique. In Sec. III we outline the numerical implementation and discuss physical results for H_2^+ strong-field ionization. Sec. IV concludes.

II. BASIC IDEAS AND PRINCIPLES

We illustrate the basic ideas and principles of the method by discussing the specific example of a linear diatomic molecules in an external electromagnetic field. In Fig. 1 we show the coordinate systems which are relevant for the field-molecule problem. The coordinates (x^L, y^L, z^L) specify the laboratory (L) fixed coordinate system defined by the external polarization vector. We assume that the field is linearly polarized and return to the generalization to elliptically polarized light in Sec. IV. The coordinate system denoted by superscripts M is the molecular fixed frame and is rotated by the Euler angles (α, β, γ) with respect to the laboratory fixed system. The rotation is accomplished by an α rotation around the z^L -axis, followed by a β rotation around the y^M -axis, and finally a γ rotation around the z^M -axis. For the case

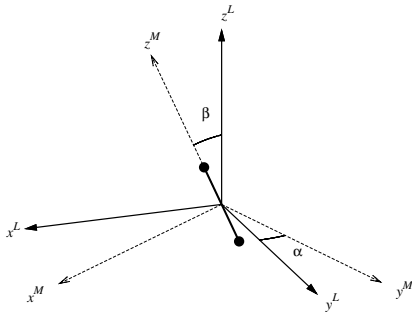


FIG. 1: The orientation of the molecular coordinate system (M , dashed) with respect to the laboratory fixed system (L , solid). In the figure only the Euler angles α, β are nonvanishing.

considered the only really distinct geometries are associated with the angle β . Results for different orientations due to the angle α are trivially related by a simple rotation around the z^L axis. Also the γ rotations around the molecular axis are insignificant as a consequence of the axial symmetry of the molecule.

We want to determine how the wave function of an electron is affected by the operators $V^{(M)}$ and $V^{(I)}(t)$, corresponding to the interaction with the nuclei and the field, respectively. We assume that we can treat these two operators separately, which is the case in a split-operator approach as described in Sec. III below. Our strategy is first to represent the wave function in the molecular frame and calculate the action of $V^{(M)}$. Secondly, we transform the updated wave function to the laboratory fixed frame and apply the operator $V^{(I)}$. Finally we can return to the molecular frame by the inverse rotation. These forward (β) and backward ($-\beta$) rotations of the wave function are illustrated in Fig. 2. The active interaction ($V^{(M)}$ or $V^{(I)}$) is marked by black and the inactive operation is gray. This propagation scheme for arbitrary orientation of the polarization axis with respect to the internuclear axis, exhibits the strength of the present approach since it allows us to perform the calculations very efficiently. Whenever we apply an axially symmetric operator, we do not mix different m states provided that the wave function is expressed in the proper reference frame. Thus we can apply the operator separately on each different m state. The decoupling of different m states means effectively that we have reduced the three-dimensional problem to a number of two-dimensional problems in addition to two rotation operations.

The rotation transformation is in principle possible in all sets of coordinates and the separation in m applies to any coordinate system where the azimuthal angle ϕ is an independent variable, e.g. cylindrical, parabolic, or spheroidal coordinates. The two unique features of the

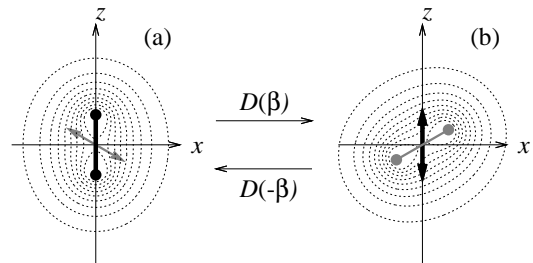


FIG. 2: Schematic picture of the rotation operation. The contour lines indicate the field free $1\sigma_g$ ground state of H_2^+ in the xz plane. The double headed arrow shows the direction of the laser polarization vector. In (a) we calculate the action of the molecular potential and express the wave function in the molecular frame with the internuclear axis parallel to the z axis. In panel (b) we transform the wave function to the laboratory fixed system with the laser polarization parallel to the z axis in order to propagate by the field interaction. The transformation between the two frames is represented by the rotation operator D .

spherical representation (1) are that (i) the transformation matrix contains Wigner rotation functions which are known analytically and (ii) the transformation is guaranteed to be exactly unitary for functions that are bandwidth limited by a maximum $l = l_{\max}$, i.e., the population in states with $l > l_{\max}$ is zero.

III. NUMERICAL RESULTS

In the present work, we solve the time-dependent Schrödinger equation (TDSE) for the electronic motion in H_2^+ in the presence of a time-dependent electromagnetic field. We represent the angular variables in a basis of spherical harmonics and write the reduced wave function as in Eq. (1). The radial functions f_{lm} which contain the time dependence are discretized on an equidistant spatial mesh. The expansion in spherical harmonics is truncated such that $l \leq l_{\max}$ leading to a total number of $(l_{\max} + 1)^2$ angular basis functions. The reduced wave function satisfies the TDSE with the Hamiltonian [atomic units ($\hbar = |e| = m_e = a_0 = 1$) are used throughout]

$$H(t) = -\frac{1}{2} \frac{\partial^2}{\partial r^2} + \frac{L^2}{2r^2} + V(t) = T_r + T_l + V(t), \quad (2)$$

where L is the usual angular momentum operator and V includes the electronic interaction with the field and the nuclei. We solve the time-evolution from time t to $t + \tau$

numerically by using the split-operator technique

$$\Phi(\mathbf{r}, t+\tau) = e^{-iT_r \frac{\tau}{2}} e^{-iT_l \frac{\tau}{2}} e^{-iV(t+\frac{\tau}{2})\tau} e^{-iT_l \frac{\tau}{2}} e^{-iT_r \frac{\tau}{2}} \Phi(\mathbf{r}, t). \quad (3)$$

The error in the propagation scheme above is approximately cubic in τ and occurs mainly due to the splitting of non-commuting operators. A related propagation scheme was applied in geometries with azimuthal symmetry [2], and the propagation techniques used for the kinetic operators T_r and T_l are readily extended to our fully three-dimensional problem. We will therefore turn to the new propagation method of the molecular potential and the field interaction.

We describe the electromagnetic field in the dipole approximation by the vector potential

$$\mathbf{A}(t) = \hat{\mathbf{e}} A_0(t) \cos(\omega t), \quad (4)$$

where $A_0(t)$ is the envelope function, ω the frequency and

$\hat{\mathbf{e}}$ the polarization direction. The electric field is obtained as $\mathbf{F}(t) = -d\mathbf{A}(t)/dt$. The operator V in Eq. (2) is written as the sum of the field interaction and the molecular potential

$$V(t) = V_{r,\theta_L}^{(I)}(t) + V_{r,\theta_M}^{(M)}, \quad (5)$$

where the subscripts denote the variables on which the operators act. θ_M is the polar angle in the molecular frame [Fig. 2 (a)] and θ_L the polar angle in the laboratory fixed system [Fig. 2 (b)]. The molecular operator is diagonal in coordinate space

$$V_{r,\theta_L}^{(M)} = V^{(M)}(r, \theta_L), \quad (6)$$

while the field interaction can be represented either in the length- (LG) or the velocity gauge (VG) as

$$V_{r,\theta_L}^{(I)}(t) = \begin{cases} F(t)r \cos \theta_L & \text{LG} \\ iA(t) \left[\frac{1}{r} \left(\cos \theta_L + \sin \theta_L \frac{\partial}{\partial \theta_L} \right) - \cos \theta_L \frac{\partial}{\partial r} \right] & \text{VG} \end{cases}. \quad (7)$$

To calculate the action of V in the propagation we make the split

$$e^{-iV(t+\frac{\tau}{2})\tau} \approx e^{-iV^{(M)}\tau/2} e^{-iV^{(I)}(t+\frac{\tau}{2})\tau} e^{-iV^{(M)}\tau/2}. \quad (8)$$

For each radial grid point r_i we write the wave function as a vector in the spherical harmonics basis, cf. Eq. (1)

$$\mathbf{f}^{(M)}(r_i, t) = \begin{pmatrix} f_{00}^{(M)}(r_i, t) \\ f_{10}^{(M)}(r_i, t) \\ \vdots \\ f_{l_{\max},0}^{(M)}(r_i, t) \\ f_{11}^{(M)}(r_i, t) \\ \vdots \\ f_{l_{\max},1}^{(M)}(r_i, t) \\ \vdots \end{pmatrix}, \quad (9)$$

where the coefficients refer to the molecular frame. The molecular potential is diagonal in the radial coordinate, and cannot induce mixings vectors that belong to different radial coordinates. We evaluate the action of $e^{-iV^{(M)}\tau/2}$ by its matrix representation in the spherical harmonics basis for each fixed value of r

$$\langle lm | e^{-iV^{(M)}\tau/2} | l'm' \rangle = \delta_{mm'} \langle lm | e^{-iV^{(M)}(r,\theta_M)\tau/2} | l'm' \rangle. \quad (10)$$

The selection rule $m = m'$ occurs since $V^{(M)}$ is independent of ϕ_M . Now it is evident that $e^{-iV^{(M)}\tau/2}$ is repre-

sented by a the block diagonal form

$$\begin{pmatrix} \begin{bmatrix} m=0 \\ l=0,1,2,\dots,l_{\max} \end{bmatrix} & & & 0 \\ & \begin{bmatrix} m=1 \\ l=1,2,\dots,l_{\max} \end{bmatrix} & & \\ & & \ddots & \\ 0 & & & \begin{bmatrix} m=l_{\max} \\ l=l_{\max} \end{bmatrix} \end{pmatrix}. \quad (11)$$

Although not essential for our present discussion, we note that for inversion symmetric potentials as in the case of H_2^+ , a further block diagonalization in even and odd parity blocks can be obtained. From the block diagonal structure of the matrix representation, it is clear that the propagation can be accomplished separately within each m subspace, and the full three-dimensional propagation effectively reduces to independent two-dimensional propagations, which can be solved by matrix multiplications on each m block. There is a total number of $2l_{\max} + 1$ individual m blocks with dimensionality between 1 and $l_{\max} + 1$.

After having applied the molecular potential we transform the wave function to the laboratory fixed frame. We relate the expansion in spherical harmonics in different frames by representation of the rotation operator in spherical harmonics, i.e., the Wigner rotation matrix $\mathbf{D}(\alpha, \beta, \gamma)$. The laboratory fixed expansion coefficients are then obtained as $\mathbf{f}^{(L)}(r_i, t) = \mathbf{D}(\alpha, \beta, \gamma) \cdot \mathbf{f}^{(M)}(r_i, t)$. We note that this matrix multiplication is very fast since the rotation does not mix different l 's and $\mathbf{D}(\alpha, \beta, \gamma)$ is

consequently sparse. Also note that the rotation operation is independent of the radial coordinate and we can therefore use the same rotation operation on all the vectors (9) for different r 's.

Having obtained the wave function in the laboratory fixed frame, we can easily apply the field interaction operator. Again, without m -couplings, the individual two-dimensional problems can be solved straightforwardly [3]. Finally we return to the molecular frame by the inverse transformation $\mathbf{f}^{(M)}(r_i, t) = \mathbf{D}^\dagger(\alpha, \beta, \gamma) \cdot \mathbf{f}^{(L)}(r_i, t)$.

We close this section with a few remarks on the scaling of the computations with the size of the problem. In an alternative three-dimensional approach where we in a single step treat the total V and mix between all $(l_{\max} + 1)^2$ angular basis states, the computational complexity scales as $O(l_{\max}^4)$ [4]. Our present method, on the other hand, scales more favourably as $O(l_{\max}^{2.7})$. In numerical simulations for typical bandwidths of $l_{\max} \sim 15 - 39$, we have checked that both three-dimensional methods agree in their predictions but with a great speed-up of the order of a factor of 100 – 500 in favor of the new method.

A. Ionization of H_2^+

We calculate the ionization probability for H_2^+ induced by a strong infra-red light source. The two protons are fixed at the equilibrium internuclear distance of 2 a.u.. The field is taken to be linearly polarized with frequency $\omega = 0.057$ a.u. ($\lambda = 800$ nm), and peak intensity 5×10^{14} W/cm². We use a sine-square envelope function that encloses seven optical cycles, corresponding to a total pulse duration of 19 fs. Convergent results are obtained with $l_{\max} = 23$ and 1024 radial grid points extending to a box size of 150 a.u.. In order to avoid reflections at the edge of the box, we impose an absorbing boundary. The time step size is $\tau = 5 \times 10^{-3}$ a.u.. We choose the velocity gauge form of the interaction since it is superior to the length gauge in producing converged results for dynamical problems [5, 6].

First we calculate the angular differential ionization probability. For that purpose we need the gauge invariant current density

$$\mathbf{J}(\mathbf{r}, t) = \text{Re} [\Psi^*(\mathbf{r}, t) (\mathbf{p} + \mathbf{A}(t)) \Psi(\mathbf{r}, t)], \quad (12)$$

where $\mathbf{p} = -i\nabla$ is the canonical momentum. We relate the outgoing radial probability flux at some large distance \mathcal{R} to the differential ionization probability in the laboratory fixed frame

$$\frac{dP}{d\Omega_L} = \int_0^\infty dt \hat{\mathbf{r}}_L \cdot \mathbf{J}(\mathcal{R}, \Omega_L, t) \mathcal{R}^2. \quad (13)$$

We must of course choose \mathcal{R} to be smaller than the radial distance at which we turn on the absorbing potential. Figure 3 shows the angular differential probabilities for the alignment angles 0° , 45° , and 90° . In all cases, the electron escapes exclusively in a very narrow cone along

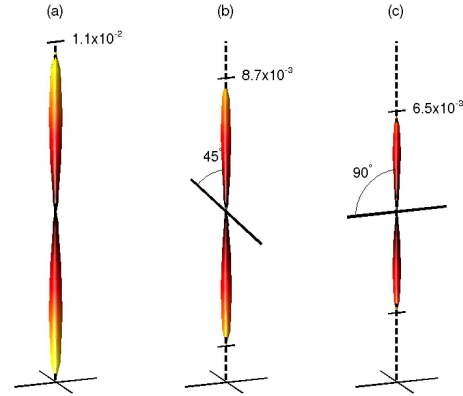


FIG. 3: (Color online) Angular differential ionization probability $dP/d\Omega_L$ for the alignment angles (a) 0° , (b) 45° , and (c) 90° . The laser polarization direction is vertical in all panels and the molecular axis is indicated by the thick solid line. The numbers on the axes indicate $dP/d\Omega_L|_{\theta_L=0}$. The parameters of the electromagnetic field are specified in the text.

the polarization direction. These results are in accordance with expectations from the quasistatic tunneling picture. The ionization dynamics is often considered as being tunneling-like for strong, low frequency fields where the Keldysh parameter fulfills $\gamma < 1$ [7]. In the present case $\gamma = 0.7$ at the peak intensity. In the tunneling picture the electron is assumed to escape near the field direction since the barrier has its shortest spatial extension in that direction [8].

The most notable difference between panels (a)-(c) is the overall scaling of the distribution which decreases with increasing angle between the polarization and internuclear axes. We can qualitatively explain this observation by the associated decrease in electronic charge density of the initial σ_g -orbital after the polarization direction (see contour plot in Fig. 2). The same reasoning carries over to the behavior of the total alignment dependent ionization probabilities shown in Fig. 4. The results in this figure can be obtained by integrating the differential ionization probability Eq. (13) over all directions. Alternatively, we may project out the bound state components of the final wave function. For comparison, Fig. 4 also contains the results from Ref. [6] which were obtained by a field of the same frequency and peak intensity but with a slightly different pulse shape (trapezoidal) and longer duration. We find somewhat lower ionization probabilities than in Ref. [6] since our pulse is at the peak intensity for a shorter duration of time. Although the two data series are not directly comparable, the overall behaviour is similar, namely decreasing ionization probability with increasing alignment angle from parallel (0°) to perpendicular (90°).

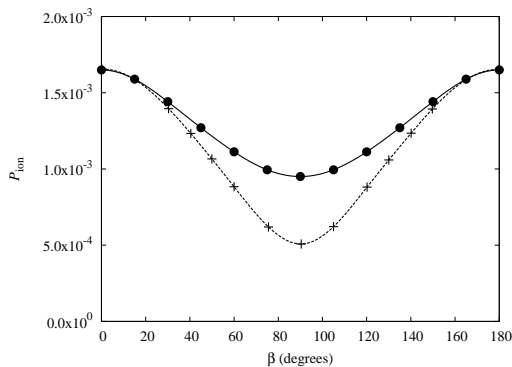


FIG. 4: Total ionization probability as a function of alignment angle. The present results are indicated by the solid line. The dashed line is taken from Ref. [6] after scaling by the factor 0.18.

IV. CONCLUSION AND OUTLOOK

In conclusion, we have developed a new approach that accurately and efficiently resolves the m -mixing problem in large scale computations in a spherical coordinate system. The method relies on an identification of rotations in the intermediate propagation that brings the wave function into a frame of reference in which m is conserved. This means that time-consuming m -mixing induced by the external perturbation is avoided and instead delegated to the rotations which are very efficiently

implemented using the Wigner rotation matrix representation of the rotation operator in the spherical harmonics basis.

We have chosen the linear molecule interacting with a linearly polarized field to illustrate our method, but a similar approach can be used in a much broader range of three-dimensional problems. For example we could consider an elliptically polarized field. In the split operator method we take the time step τ to be small enough such that the field can be taken to be constant both in magnitude and polarization direction within the small time interval. We can therefore consider a time-dependent laboratory frame which follows the instantaneous polarization direction. If we make the transformation from the molecular frame to the new laboratory frame, we are again able to treat the field as being linear and propagate as discussed above. Our method can also be extended to arbitrary nuclear positions. For any nuclear configuration, we can attach a coordinate system to each nucleus with a z axis from the origin to the nucleus. Then we decompose the molecular potential to a sum of nuclear potentials, each of which can be propagated with azimuthal symmetry in their own reference frame. Despite the fact that we now need rotations between the coordinate systems belonging to all of the nuclei, the total calculation is still in the same complexity class with respect to scaling in l_{max} .

This work is supported by the Danish Research Agency (Grant. No. 2117-05-0081).

-
- [1] F. Martin, J. Phys. B **32**, R197 (1999).
 - [2] M. R. Hermann and J. A. Fleck, Phys. Rev. A **38**, 6000 (1988).
 - [3] D. Bauer and P. Koval, Comp. Phys. Comm. **174**, 396 (2006).
 - [4] J. P. Hansen, T. Sorevik, and L. B. Madsen, Phys. Rev. A **68**, 031401(R) (2003).
 - [5] E. Cormier and P. Lambropoulos, J. Phys. B **29**, 1667 (1996).
 - [6] G. L. Kamta and A. D. Bandrauk, Phys. Rev. A **71**, 053407 (2005).
 - [7] L. V. Keldysh, Sov. Phys. JETP **20**, 1307 (1965).
 - [8] B. M. Smirnov and M. I. Chibisov, Sov. Phys. JETP **22**, 585 (1966).